

Ultracompact plasmonic racetrack resonators in metal-insulator-metal waveguides

Z. Han

Department of electrical and computer engineering, University of Alberta, Edmonton,

T6G2V4, Canada

zhanghua@ualberta.ca

Abstract-Among various plasmonic waveguides, the metal-insulator-metal (MIM) type is the most promising for true subwavelength photonic integration. To date, many photonic devices based on MIM waveguides have been investigated, including resonators. However, most of the reported MIM ring resonators suffer from low extinction ratios. In this paper, we present a comprehensive analysis of the intrinsic reasons for the low performance of MIM ring resonators, and give the analytical transmission relation for a universal all-pass ring resonator which has coupling loss. Based on the analysis we propose the plasmonic racetrack resonators in MIM waveguides and show that the performance can be greatly improved.

Keywords: Surface plasmons; ring Resonators; plasmonics

1. Introduction

Plasmonic waveguides [1] have recently attracted much attention due to their ability to confine light beyond the diffraction limit, therefore potentially enabling device integration on a scale which is not accessible with conventional dielectric waveguides or photonic crystal waveguides. To date, various plasmonic waveguide structures have been proposed [2-5] and investigated for planar photonic integration. In general most plasmonic waveguides can be classified into three basic types: insulator-metal-insulator (IMI), insulator-metal (IM) and metal-insulator-metal (MIM). In optical regime especially in the infrared, light in IMI and IM types of plasmonic waveguides may penetrate into the insulator for several wavelengths. So these two types of plasmonic waveguides can hardly provide true sub diffraction confinement while MIM type can when the width of the insulator is very small and in principle there is even no cut off. Thus MIM type of plasmonic waveguides is the ideal candidate for true subwavelength photonic integration, albeit the loss with MIM waveguides is a bit larger than the other two types.

To realize subwavelength photonic integration based on the plasmonics platform, people not only need to guide the light with nano scale confinement, but also need to realize much functionality, e.g. filtering, routing and multiplexing, on the same platform. One of the devices that can provide such functionality is a resonator, which can exhibit some resonant behaviors and function on certain wavelengths from a signal. Bragg grating type of resonators in the MIM waveguides were investigated in the literature [6]; however, these devices suffer from a relatively large length because a number of Bragg periods are needed. The recently

proposed Tooth-shaped plasmonic waveguide filter [7] is shorter, but the bandwidth is too large for the filtering application.

Considering the fact that light can propagate through sharp bending in MIM waveguides with high transmission [3] [8], MIM waveguides will be perfect candidates for constructing ring resonators, in which the bending loss is negligible and ring resonators with subwavelength radius can be achieved. In ref [9] plasmonic ring resonators based on circular geometries were theoretically investigated and ring resonators based on channel plasmonic waveguides were reported in ref [5]. However, we find that all these resonators suffer from a relatively low extinction ratio. To show one of these results, Fig.1 gives the calculated transmission spectrum for a MIM ring resonator with a radius 500nm evanescently coupled to a MIM bus waveguide using the finite-difference time-domain (FDTD) method [10] with convolutional perfectly matched layer (CPML) boundary conditions. The index of the insulator is assumed to be 1.45, the typical index value of SiO_2 or some polymers in the infrared. The metal is silver, with the permittivity described by Drude model $\varepsilon_r = \varepsilon_\infty - \omega_p^2 / (\omega^2 + j\gamma\omega)$, with $\varepsilon_\infty = 3.7$, $\omega_p = 9.1\text{eV}$ and $\gamma = 0.018\text{eV}$, which were obtained by fitting the experimental data [11] for silver permittivity in the infrared frequencies. Both the bus waveguide and the ring resonator have an insulator width 100nm and the gap between them is 25nm, which we think is possible to realize and control with the state of art electron beam lithography or focused ion beam lithography fabrication facilities.

From Fig.1 we can see that in the range between $1\mu\text{m}$ and $2.25\mu\text{m}$, the extinction ratio for this regular MIM ring resonator is very small, less than 5dB. The low extinction ratio limits the application of this ring resonator, and the reasons for the low extinction ratios have

not been analyzed in the literature. In part 2 of this paper, we will give a comprehensive analysis of the reasons why the extinction ratio is so small. We note that although in ref [12], the transmission in a universal all pass ring resonator is given; however, it is assumed therein that there is no loss in the coupling region, which is not true in the plasmonic case. In that part we give our analysis for a more universal all pass ring resonators where loss exists in the coupling region. Based on the analysis, we propose a MIM racetrack resonator in part 3 and show that the performance can be significantly improved. The whole paper concludes in part 4. We note here that although the proposal in part 3 is focused on MIM waveguides, it can be extended to other plasmonic waveguide systems. What's more, the analysis in part 2 are not restricted to MIM resonators, but applicable for any resonators and the analysis can be used as a guideline for the design of all kinds of plasmonic resonators with high performances.

2. Analysis

The schematic of a universal all-pass ring resonator is shown in Fig.2. When the coupling region has loss and non-zero physical length, the coupling coefficient κ and transmission coefficient $\tau = |\tau|e^{i\phi_r}$ are both complex numbers, and we assume $|\tau|^2 + |\kappa|^2 = \beta$, which may not equal to 1 any more. The coupling relation can be described by the matrix:

$$\begin{vmatrix} b_1 \\ b_2 \end{vmatrix} = \begin{vmatrix} \tau & \kappa \\ -\kappa^* & \tau^* \end{vmatrix} \begin{vmatrix} a_1 \\ a_2 \end{vmatrix} \quad (1)$$

And the transmission around the resonator is given by

$$a_2 = \alpha e^{i\theta} b_2 \quad (2)$$

where real number α is the inner circulation factor to describe the internal loss, equaling to 1 when there is no internal loss, and θ is the round trip phase.

From (1) and (2), we can get:

$$b_1 = \frac{-\alpha\beta a_1 + \tau e^{-i\theta} a_1}{-\alpha\tau^* + e^{-i\theta}} \quad a_2 = \frac{-\alpha\kappa^*}{-\alpha\tau^* + e^{-i\theta}}$$

So the transmission is:

$$T = \frac{|b_1|^2}{|a_1|^2} = \frac{\beta^2\alpha^2 + |\tau|^2 - 2\alpha\beta|\tau|\cos(\theta + \phi_\tau)}{1 + \alpha^2|\tau|^2 - 2\alpha|\tau|\cos(\theta + \phi_\tau)} \quad (3)$$

From equation (3) one knows that the transmission at resonance ($\theta + \phi_\tau = 2m\pi$, m is an integer) is:

$$T = \frac{(\alpha\beta - |\tau|)^2}{(1 - \alpha|\tau|)^2} \quad (4)$$

So the condition of critical coupling in ref [12] is now changed to $\alpha\beta = |\tau|$, which determines the extinction ratio for a universal all-pass resonator. Compared to dielectric ring resonators, plasmonic waveguides suffer from more loss in the ring and there is also some loss in the coupling region, showing that α and β are relatively smaller than in the dielectric counterparts ($\beta=1.0$ for dielectric waveguide). What's more, $|\tau|$ is larger in the plasmonic case because more power goes through the straight bus waveguide due to the weak coupling. The two reasons make the deviation between $\alpha\beta$ and $|\tau|$ for plasmonic resonator larger than that for dielectric resonators. This is the origin of the low extinction ratio for MIM plasmonic resonators. In the following part, we will give the specific values of them and show the deviation.

The key to increase the extinction ratio of MIM ring resonators is to reduce the deviation between $\alpha\beta$ and $|\tau|$ at resonant wavelengths. Some approaches, e.g. aperture-coupling [13], have been proposed to fulfill this requirement. Considering the fact that light coupling between two waveguides is proportional to the coupling length, we propose in this paper

MIM ring resonators with increased coupling length, i.e. plasmonic racetrack resonators in the MIM waveguides.

We first show how the deviation between $\alpha\beta$ and $|\tau|$ can be alleviated in the racetrack resonator at 1550nm. For simplicity, we assume the effective index in the bending MIM

waveguide is the same as the straight MIM waveguide, so α equals to $e^{-\frac{2\pi n'' L_r}{\lambda_0}}$, where λ_0 is the free space wavelength 1550nm, n'' is the imaginary part of the effective index in the MIM waveguides, L_r is the round trip length in the racetrack resonator and $L_r = 2(\pi R + L)$ where R is the radius of the ring and L is the length of the coupling region.

By solving the dispersion equation of a MIM waveguide at 1550nm with the insulator width 100nm and index 1.45, we can find $n_{eff} = n' + n''j = 1.747 + 0.00327j$. So the relation between α in the racetrack resonator and L can be obtained. To calculate τ , κ and β , we separate the coupling region from the resonator, shown as the inset in Fig. 3(a) and FDTD is used to calculate those parameters. The material parameters are the same as given above, and a continuous wave at 1550nm is incident from the left port of straight waveguide. When the simulation becomes stable, the magnetic fields at planes A and B are used to calculate τ , κ and the magnetic field at plane A when there is no upper waveguide is used as the reference. Fig. 3(a) gives the result for τ and κ as well as $\alpha\beta$ for different coupling lengths.

From the result we can see that as the length increases, the coupling between the two waveguide becomes stronger and the deviation between τ and $\alpha\beta$ becomes less. When the length L reaches approximately 670nm, τ equals to $\alpha\beta$ and when L exceeds 670nm, the deviation between τ and $\alpha\beta$ starts to increase again, meaning a state of “over coupling” now. Fig. 3(a) also shows that when L equals to 0, the case for the coupling in a circular plasmonic

resonator as shown as inset in Fig. 1, τ is 0.9922 while $\alpha\beta$ is 0.9551, so according to equation (4), at resonance T equals to 59.1% or -2.3 dB. This result is consistent with the result shown in Fig. 1 obtained with FDTD method.

3. Proposal and numerical results.

The result in Fig.3 (a) inspires an idea that when the length of the coupling region approaches 670nm, a state close to critical coupling can be realized and this can be used to design a resonator with a much higher extinction ratio. The schematic of such a plasmonic resonator with increased coupling length, or racetrack plasmonic resonator, is shown as the inset in Fig 3(b). FDTD method is used again here and the calculated result is shown in Fig. 3(b). One sees that the extinction ratio around $1.55\mu\text{m}$ has been significantly increased from less than 3dB to around 35dB now. It is also seen in Fig. 3(b) that the extinction ratio for other resonant waveguides within the range between $1\mu\text{m}$ and $2.25\mu\text{m}$ is also increased, although not so significant as it for the wavelength around $1.55\mu\text{m}$, indicating the condition for critical coupling is less fulfilled for those wavelengths. Considering that the coupling is weaker for longer wavelengths, we believe that it is under-coupling ($\alpha\beta<\tau$) for wavelengths longer than $1.6\mu\text{m}$ and over-coupling ($\alpha\beta>\tau$) for wavelengths shorter than $1.4\mu\text{m}$.

We find that compared to the result of $\Delta\lambda_{\text{FWHM}}$ (full width at half maximum) in Fig. 1 at around resonant wavelength $1.386\mu\text{m}$ to be 8.1nm , $\Delta\lambda_{\text{FWHM}}$ for the racetrack resonator is about 11nm around resonant wavelength $1.308\mu\text{m}$. Considering that $\Delta\lambda_{\text{FWHM}} = \frac{\lambda^2}{\pi n_{\text{eff}} L_{\text{rt}}} \frac{1-\alpha\tau}{\sqrt{\alpha\tau}}$ [14], the slight increase of $\Delta\lambda_{\text{FWHM}}$ with racetrack resonator means the decrease of τ plays a more important role than the increase of L_{rt} . We also find that the free

spectral range (FSR) at around $1.55\mu\text{m}$ in the racetrack resonator is larger than that in the circular resonator, which we believe is mainly due to an increase of L_{rt} .

One may also notice that the extinction ratio for the resonant wavelength around $1.55\mu\text{m}$ is only 34dB while from equation (4) this number should be even higher. Besides the numerical errors and the fact that the effective index for a straight MIM waveguide is used for simplicity for the bending MIM waveguide, the main reason for this is because the result shown in Fig. 3(a) is calculated for the $1.55\mu\text{m}$ wavelength while the resonant wavelength around $1.55\mu\text{m}$ in Fig. 3(b) is precisely $1.565\mu\text{m}$. The small difference between $\alpha\beta$ and τ for $1.565\mu\text{m}$ degrades the extinction ratio a bit and this can be improved by carefully designing the plasmonic racetrack resonator geometry to fulfill the phase condition and critical coupling condition at the same time. For the result shown in Fig. 3(b), we note that the length 670nm is still relatively short compared to the resonant wavelength and the overall size of the plasmonic racetrack resonator is still very small.

Fig.4 (a) gives a snapshot of the magnetic field profile in the whole plasmonic racetrack resonator system for the resonant wavelength $1.565\mu\text{m}$. As can be seen straightforwardly in the figure, the field in the output port of the bus waveguide is very weak, showing that the lights meeting here have a destructive interference. To assess the sensitivity of the extinction ratio to the length error of the coupling region, we performed a set of simulations, in which the length of the coupling region has some deviations from 670nm. Fig. 4(b) shows the extinction ratios under different length errors at around wavelength $1.55\mu\text{m}$. Please note that the resonant wavelengths have changed a bit from $1.565\mu\text{m}$ because L_{rt} has changed. As is seen, the extinction ratio is slightly degraded, which can be easily understood because the

coupling is away from the critical coupling discussed in part 2. However, the extinction ratio is still much higher (>20dB) than the result of the circular MIM resonators.

4. Conclusion

In a summary, we presented in this paper a comprehensive analysis of the poor performance for a circular plasmonic ring resonator, gave the transmission relation in a universal all-pass resonator where coupling loss exists and then proposed and investigated the racetrack MIM resonators. The simulation results show that the proposed racetrack resonators have significant improvement in extinction ratio over the circular MIM ring resonator. Although we focus on plasmonic resonators based on MIM waveguides as an example, our analysis can be used as a guideline for the design of all kinds of high performance plasmonic resonators. Besides the all-pass resonator, the idea of racetrack MIM resonators can be extended to other resonator systems, e.g. add-drop plasmonic resonator and find extensive applications in the field of plasmonic devices. These devices will help to realize much functionality on the plasmonics platform.

Acknowledgments

This work was supported by the Natural Sciences and Engineering Research Council of Canada.

References

- [1] W. L. Barnes, A. Dereux, and T. W. Ebbesen, "Surface plasmon subwavelength optics", *Nature*, 424, 824-830 (2003).
- [2] P. Berini, "Plasmon-polariton waves guided by thin lossy metal films of finite width: Bound modes of symmetric structures", *Phys. Rev. B*, 61, 10484-10503 (2000).
- [3] L. Liu, Z. Han and S. He, "Novel surface plasmon waveguide for high integration", *Opt. Express*, 13, 6645-6650 (2005).
- [4] A. V. Krasavin and A. V. Zayats, "Passive photonic elements based on dielectric-loaded surface plasmon polariton waveguides", *Appl. Phy. Lett*, 90, 211101 (2007).
- [5] S. I. Bozhevolnyi, V. S. Volkov, E. Devaux, J.-Y. Laluet, and T. W. Ebbesen, "Channel plasmon subwavelength waveguide components including interferometers and ring resonators", *Nature* 440, 508-511 (2006).
- [6] Z. Han, E. Forsberg a nd S. He, "Surface Plasmon Bragg Gratings Formed in Metal-Insulator-Metal Waveguides", *IEEE. Photon. Tech. Lett*, 19, 91-93 (2007).
- [7] X. Lin and X. Huang, "Tooth-shaped plasmonic waveguide filters with nanometeric sizes," *Opt. Lett.* 33, 2874-2876 (2008).
- [8] G. Veronis and S. Fan, "Bends and splitters in metal-dielectric-metal subwavelength plasmonic waveguides", *Appl. Phys. Lett*, 87, 131102 (2005).
- [9] S. Xiao, L. Liu and M. Qiu, "Resonator channel drop filters in a plasmon-polaritons metal", *Opt. Express*, 14, 2932-2937 (2006).
- [10] Taflove and S. C. Hagness, *Computational Electrodynamics: The Finite-Difference Time-Domain Method*, 3rd ed. (Artech House, Boston, 2005).

[11]P. B. Johnson and R. W. Christy, “Optical constants of the noble metals,” Phys. Rev. B, vol. 6, no. 12, pp. 4370–4379, 1972.

[12]A. Yariv, “Universal relations for coupling of optical power between microresonators and dielectric waveguides”, Electron. Lett, 36, 321-322 (2000).

[13]Z. Han, V. Van, W. N. Herman and P. T. Ho, “Aperture-coupled MIM plasmonic ring resonators with sub-diffraction modal volumes”, Opt. Express, 17(15), 12678-12684 (2009).

[14]Kuldeep Amarnath, “Active Microring and Microdisk Optical Resonator on Indium Phosphide”, PhD dissertation, University of Maryland, College Park (2006).

List of Figures:

Fig.1 Calculated transmission spectrum with FDTD for a plasmonic ring resonator; Inset: schematic of a MIM ring resonator side coupled to a MIM bus waveguide, yellow region: metal and brown region: insulator. R: 500nm, G: 25nm and W: 100nm.

Fig.2 Schematic of a universal all-pass ring resonator with coupling loss.

Fig. 3 (a) the magnitudes of transmission coefficient $|T|$ and coupling coefficient $|C|$ versus the length of the coupling region; Inset: Schematic of the coupling region, yellow region: metal and brown region: insulator. R: 500nm, G: 25nm and W: 100nm; (b) Calculated transmission spectrum with FDTD method for the plasmonic racetrack resonator; Inset: Schematic of the plasmonic racetrack resonator, brown region: metal, brown region: insulator. R: 500nm, L: 670nm, W: 100nm and G: 25nm.

Fig. 4 (a) the magnetic field profile for the wavelength 1565nm; (b) Extinction ratios versus the errors of the length of coupling region.

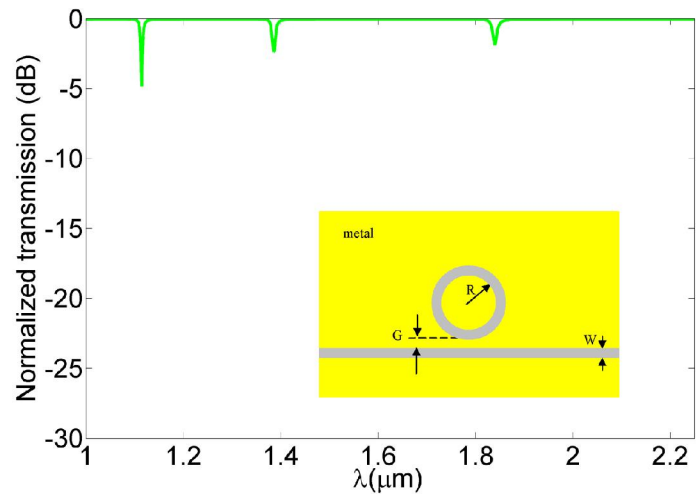


Fig.1 Calculated transmission spectrum with FDTD for a plasmonic ring resonator; Inset: schematic of a MIM ring resonator side coupled to a MIM bus waveguide, yellow region: metal and brown region: insulator. R: 500nm, G: 25nm and W: 100nm.

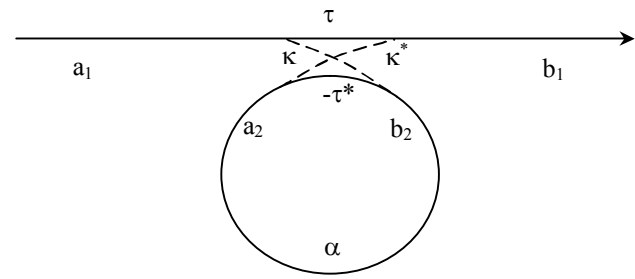
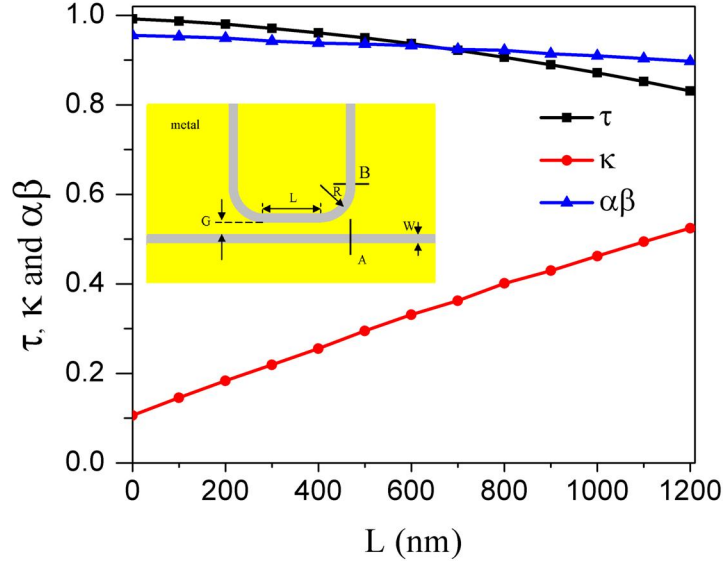
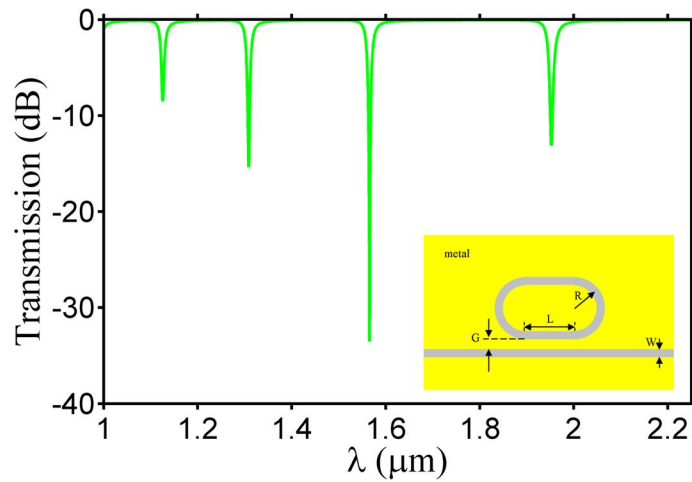


Fig.2 Schematic of a universal all-pass ring resonator with coupling loss.

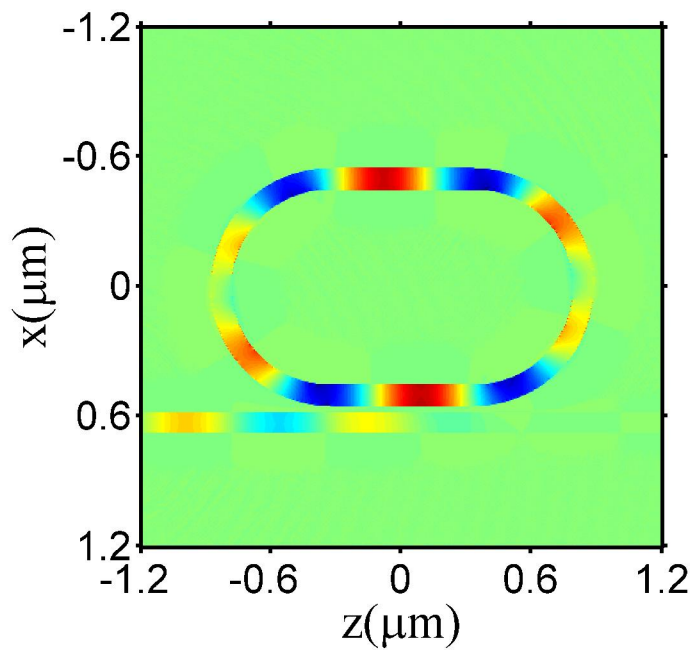


(a)

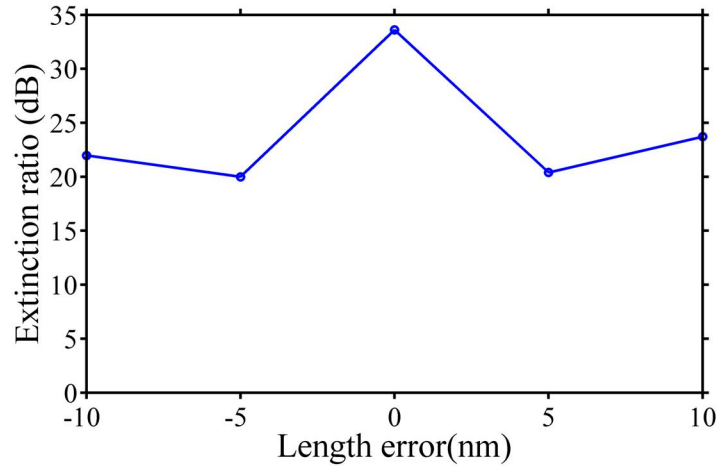


(b)

Fig. 3 (a) the magnitudes of transmission coefficient τ and coupling coefficient κ and $\alpha\beta$ versus the length of the coupling region; Inset: Schematic of the coupling region, yellow region: metal and brown region: insulator. R: 500nm, G: 25nm and W: 100nm; (b) Calculated transmission spectrum with FDTD method for the plasmonic racetrack resonator; Inset: Schematic of the plasmonic racetrack resonator, brown region: metal, brown region: insulator. R: 500nm, L: 670nm, W: 100nm and G: 25nm.



(a)



(b)

Fig. 4 (a) the magnetic field profile for the wavelength 1565nm; (b) Extinction ratios versus the errors of the length of coupling region.